jmb Communication

Electron Microscopy and 3D Reconstruction Reveals Filamin Ig Domain Binding to F-Actin

Worawit Suphamungmee[1], Fumihiko Nakamura[2], John H. Hartwig[2] and William Lehman[1]

*1 - **Department of Physiology and Biophysics,** Boston University School of Medicine, 72 East Concord Street, Boston, MA 02118, USA*
*2 - **Translational Medicine Division,** Department of Medicine, Brigham and Women's Hospital, Harvard Medical School, One Blackfan Circle, Boston, MA 02115, USA*

Correspondence to William Lehman: *wlehman@bu.edu*
http://dx.doi.org/10.1016/j.jmb.2012.09.025
Edited by M. Moody

Abstract

Filamin A (FLNa) is an actin-binding protein that cross-links F-actin into networks of orthogonally branched filaments. FLNa also directs the networks to integrins while responding to mechanochemical signaling pathways. Flexible, 160-nm-long FLNa molecules are tail-to-tail dimers, each subunit of which contains an N-terminal calponin homology (CH)/actin-binding domain connected by a series of 24 immunoglobulin (Ig) repeats to a dimerization site at their C-terminal end. Whereas the contribution of the CH domains to F-actin affinity is weak (apparent $K_a \sim 10^5$), the binding of the intact protein to F-actin is strong (apparent $K_a \sim 10^8$), suggesting involvement of additional parts of the molecule in this association. Indeed, previous results indicate that Ig repeats along FLNa contribute significantly to the strength of the actin filament interaction. In the current study, we used electron microscopy and three-dimensional reconstruction to elucidate the structural basis of the Ig repeat–F-actin binding. We find that FLNa density is clearly delineated in reconstructions of F-actin complexed either with a four-Ig-repeat segment of FLNa containing Ig repeat 10 or with immunoglobulin-like filamin A repeat (IgFLNa)10 alone. The mass attributable to IgFLNa10 lies peripherally along the actin helix over the N-terminus of actin subdomain 1. The IgFLNa10 interaction appears to be specific, since no other individual Ig repeat or fragment of the FLNa molecule examined, besides ones with IgFLNa10 or CH domains, decorated F-actin filaments or were detected in reconstructions. We conclude that the combined interactions of CH domains and the IgFLNa10 repeat provide the binding strength of the whole FLNa molecule and propose a model for the association of IgFLNa10 on actin filaments.

The cortical cytoskeleton regions of virtually all eukaryotic cells contain highly dynamic networks of actin filaments. The networks model and remodel in order to control cell shape and motility, while responding to intracellular and/or extracellular chemical and mechanical signals.[1–3] Typically, signaling pathways lead to the binding or dissociation of members of a group of well over 100 distinct actin-binding proteins, which in turn specify the restructuring of the actin cytoskeleton.[4] Some actin-binding proteins nucleate, sever, or depolymerize filaments, thus regulating F-actin growth or disassembly. Others cross-link F-actin into tight bundles or looser networks, thus transforming cell superstructure and plasticity.[1–4] Bivalent filamin A (FLNa), the first non-muscle actin-binding protein to be identified[5] and the subject of our investigation, cross-links neighboring F-actin in cells into arrays of orthogonally oriented filaments[6] while at the same time presenting surface domains for protein partner interactions that are primed to transform the resulting filament network further.[7–11]

The C-terminal ends of elongated FLNa subunits self-associate to form a flexible V-shaped homodimer. The tips of the resulting structure, at the N-

termini of the dimerized chains, contain paired calponin homology (CH) domains (a.k.a. actin-binding domains or ABDs), which are conserved modules found in many actin-binding proteins.[12] They contribute, at least partially, to the actin-binding function of FLNa, and their presence at the two ends of the dimer can account for FLNa–F-actin cross-linking.[8,10,13]

Each N-terminal CH domain/ABD is separated from the C-terminal dimerization site by an ~80-nm-long set of 24 Ig segments arranged in tandem. Hinge domains separating Ig repeats 15 and 16 as well as repeats 23 and 24 provide molecular flexibility. Pairing between repeats 16–17, 18–19, and 20–21 generates a globular C-terminal domain that can be distended by mechanical forces.[14,15] Binding studies show that FLNa CH-domain constructs, like other members of the "spectrin ABD superfamily", interact with F-actin with very low affinity ($K_d \sim 1.7\times10^{-5}$ M); however, the intact full-length FLNa dimer binds actin filaments with considerably higher avidity ($K_d \sim 1.7\times10^{-8}$ M).[8,10] Hence, other regions of the molecule, presumably the FLNa Ig repeats, are likely to contribute to the binding strength of intact FLNa for F-actin.[8,10] In fact, Ig repeats in muscle proteins such as paladin,[16,17] kettin,[18,19] myosin-binding protein C,[20–22] and titin[23] all have been reported to interact with F-actin.

In our previous work, a library of FLNa fragments was generated and used to characterize filamin–actin binding by F-actin co-sedimentation.[8] This work showed that constructs including both FLNa Ig repeats 9–15 and the FLNa CH domains displayed F-actin binding comparable to that of the full-length protein, suggesting a role for Ig repeat–actin interaction.[8] However, the studies did not categorize the binding site on FLNa further or locate the Ig-binding target on actin. In order

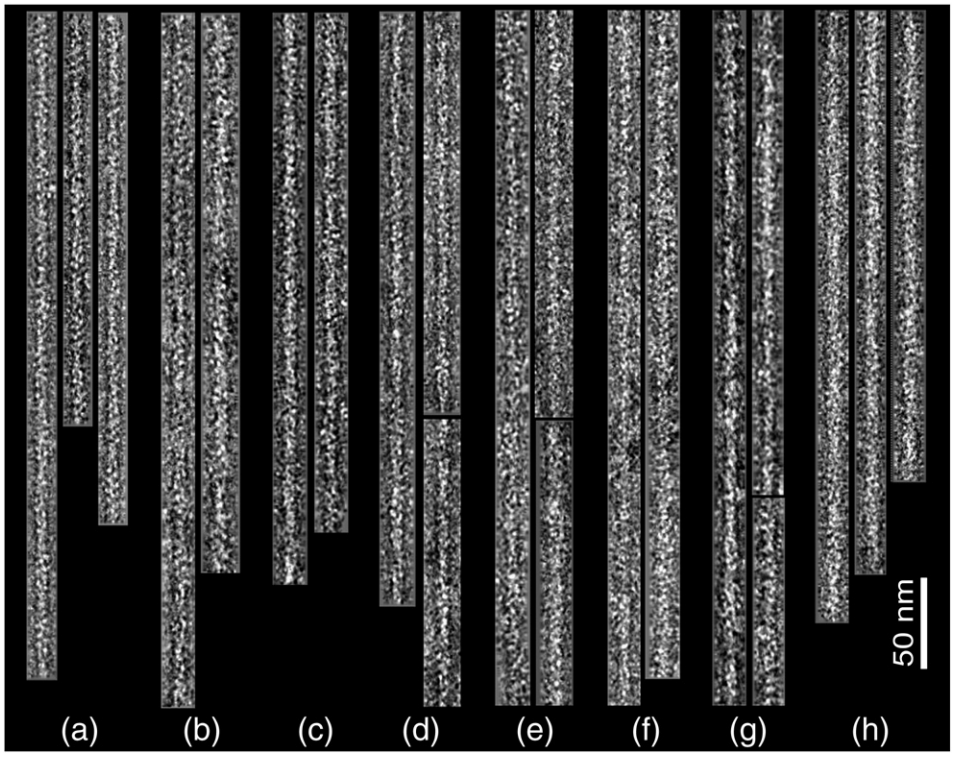

Fig. 1. Electron micrographs of negatively stained filaments. (a) F-actin control. (b–h) F-actin mixed with various FLNa constructs: (b) IgFLNa10, (c) IgFLNa9, (d) IgFLNa17, (e) IgFLNa8–11, (f) IgFLNa12–15, (g) IgFLNa16–23, and (h) ABD-FLNaIg1–4. The scale bar represents 50 nm. *Protein preparation*: F-actin was polymerized and isolated as previously described.[25] FLNa constructs were expressed and purified as in Ref. 8. *Electron microscopy*: EM work was carried out on filaments prepared by adding a fivefold molar excess of a particular FLNa construct to F-actin (20 μM) in the case of single Ig-repeat constructs and twofold molar excess for multidomain constructs. Samples were mixed in 100 mM NaCl, 3 mM $MgCl_2$, 1 mM NaN_3, 0.2 mM ethylene glycol bis(β-aminoethyl ether)*N*,*N*′-tetraacetic acid, 1 mM dithiothreitol, and 5 mM sodium phosphate/5 mM Pipes buffer (pH 7.0) at 25 °C.[26] These conditions were chosen to balance favorable binding of constructs and F-actin against background interference resulting from excess unbound protein; when higher ratios of FLNa were used, background noise tended to preclude satisfactory image processing and 3DEM. The above mixtures of F-actin and FLNa constructs were diluted 20-fold, quickly applied to carbon-coated grids, and stained with 1% uranyl acetate.[26] EM was performed on a Philips CM120 EM at a magnification of 45,000× under low-dose conditions (~12 $e^-/Å^2$).

to define filamin–actin association more completely, we have now examined potential binding interactions of Ig domains structurally by electron microscopy (EM) and three-dimensional (3D) reconstruction. Here, F-actin filaments mixed either with multidomain FLNa fragments or with single Ig

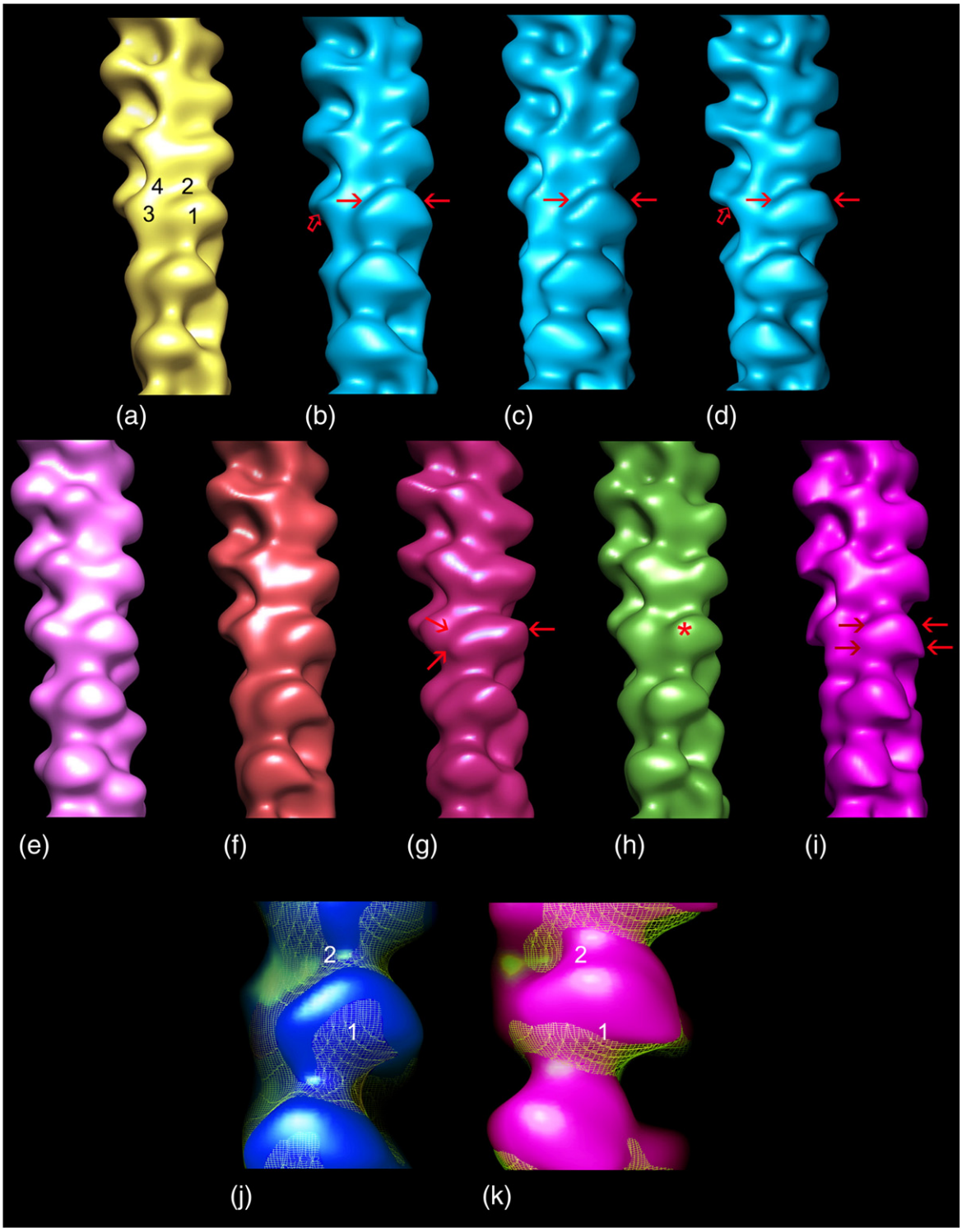

Fig. 2 (*legend on next page*)

repeats were studied. 3DEM (3D reconstruction of EM images) of complexes containing Ig repeat 10 (a mutational hot spot)[24] showed distinct densities attributable to the Ig domain, which is bound over the N-terminus of actin subdomain 1. FLNa constructs, besides those containing immunoglobulin-like filamin A repeat (IgFLNa)10 or CH domains, did not show obvious signs of F-actin labeling. The general significance of our findings is discussed.

EM of F-actin–IgFLNa complexes

Long FLNa fragments containing six to eight Ig repeats, particularly those with N-terminal CH domains, bundle F-actin and were not suitable for further analysis. Four relatively short FLNa constructs, which represent most of the molecule (viz., FLNa segments: IgFLNa8–11, IgFLNa12–15, IgFLNa16–23, and ABD-FLNaIg1–4), were chosen for study since they do not bundle F-actin. In addition, individually expressed Ig repeats 9, 10, and 17 were examined [IgFLNa9, IgFLNa10, and IgFLNa17 (nomenclature from Ref. 8)]. All constructs were mixed with 1 μM F-actin in 2–5:1 molar excess (molar ratio to actin subunits) to promote effective binding without causing significant protein background interference in electron microscope images. Electron micrographs of negatively stained samples confirmed that none of these constructs cross-link F-actin, and thus, the filaments observed were well separated from each other as required for subsequent analysis. Direct inspection of the micrographs suggested an increased filament diameter brought about by the presence of, for example, fragments IgFLNa8–11, ABD-FLNaIg1–4, and IgFLNa10 (Fig. 1). However, no discrete structures derived from FLNa were obvious in any of the micrographs; hence, 3D image alignment and reconstruction were required to characterize potential binding interactions in the filaments.

3D reconstructions of F-actin–IgFLNa complexes

Reconstructions generated from FLNa-labeled F-actin reveal well-demarcated, helically arranged actin subunits and clearly defined actin subdomain structure (Fig. 2). Additional mass is seen on the surface of F-actin in reconstructions of mixtures containing IgFLNa10 and IgFLNa8–11 (Fig. 2b and g, arrows). These extra densities are present on the "top" of subdomain 1 of each actin subunit. The IgFLNa10 label forms a fairly compact density that caps subdomain 1, which partially obscures subdomain 2 (Figs. 2b and j and 4a). The mass formed by IgFLNa8–11, the four-repeat fragment containing IgFLNa10, displays broader extra density on the upper aspect of actin subdomain 1 that extends across subdomain 1 in the direction of subdomain 3 (Fig. 2g, arrows). In contrast, F-actin decorated with constructs representing Ig repeats 12–15 (Fig. 2h) or 16–23 (not shown) does not show signs of extra density on actin subunits; neither do single Ig repeats 9 and 17 show structural evidence of binding (Fig. 2e and f). As expected, the mixed domain construct consisting of the FLNa CH-domain ABD and, in the case tested, the first four FLNa Ig repeats (ABD-IgFLNa1–4) does indicate F-actin labeling, evidently derived from the CH-domain interactions on F-actin (Fig. 2i and k), corroborating previous reports on the structural binding of FLNa CH domain

Fig. 2. Surface views of thin filament 3D reconstructions. (a) Reconstruction of F-actin control filaments (subdomains noted on one actin subunit). (b–i) Reconstructions of F-actin–FLNa mixtures containing (b–d) IgFLNa10, (e) IgFLNa9, (f) IgFLNa17, (g) IgFLNa8–11 (h) IgFLNa12–15, and (i) ABD-FLNaIg1–4. Note extra density (red arrows) on subdomain 1 of actin subunits in reconstructions of F-actin decorated with (b) IgFLNa10, (g) IgFLNa8–11, and (i) ABD-FLNaIg1–4. Such extra density is not observed in reconstructions of F-actin (e) IgFLNa9 and (f) IgFLNa17 or (h) IgFLNa12–15 mixtures. A trace of extra density (asterisk) may be present on subdomain 1 in (h) F-actin–IgFLNa12–15. Reconstructions of F-actin–IgFLNa16–23 were poorly delineated, but extra densities were not apparent (not shown). A very small pointed density is detected on the periphery of the inner aspect of actin in IgFLNa10-decorated maps (open red arrow). Reconstructions in (c) and (d) represent maps of F-actin–IgFLNa10, each derived from half the data comprising the reconstruction shown in (b). (j and k) Here, reconstructions of F-actin filaments decorated with (j) IgFLNa10 (blue) and (k) ABD-FLNaIg1–4 (magenta) are superposed over F-actin (yellow wire mesh). These images are enlargements of reconstructions in (b) and (i) above, rotated to display the outer domain of an actin subunit (subdomains 1 and 2 noted). FLNa association on F-actin is evident in (j) from the ridge of density on the top of subdomain 1 and in (k) from the shelf of density on subdomain 1, which extends to subdomain 2. All of the reconstructions of thin filaments obtained were aligned to each other and are shown with filament pointed ends facing up. Helical reconstruction was performed as previously described[27,28] by using standard computational methods documented in the Brandeis Helical Package.[29] The methods yield the angular displacement between actin monomers along the F-actin genetic helix (F-actin alone, 166.4±0.25°; F-actin–IgFLNa10, 166.4±0.61°; F-actin–IgFLNa9, 166.4±0.38°; F-actin–IgFLNa17, 166.7±0.23°; F-actin–IgFLNa8–11, 166.6±0.29°; F-actin–IgFLNa12–15; 166.3±0.40°, F-actin–ABD-IgFLNa1–4, 166.5±0.18°). Hence, the data show that the average twist of the F-actin helix is unaffected by the presence of the FLNa constructs. The number of filaments used to generate each of the reconstructions shown was as follows: F-actin, 22; F-actin–IgFLNa10, 12; F-actin–IgFLNa9, 7; F-actin–IgFLNa17, 7; F-actin–IgFLNa8–11, 12; F-actin–IgFLNa12–15, 6; F-actin–ABD-IgFLNa1–4, 9.

to actin.[33] None of the constructs tested changed the average twist values of the actin filament (noted in Fig. 2), which is consistent with previous results indicating that phalloidin does not interfere with filamin binding to F-actin.[34]

Statistical analysis of reconstructions of the F-actin–IgFLNa10 complex

The densities contributing to the F-actin–IgFLNa10 reconstructions, including those derived from IgFLNa10, are statistically significant at 95–99% confidence levels. Moreover, IgFLNa10 contribution can also be identified as discrete "difference densities" when maps of control pure F-actin are subtracted from those of F-actin–IgFLNa10 filaments (Fig. 3a and b). These difference densities fall within outlines of the F-actin–IgFLNa10 reconstruction and are themselves statistically significant at greater than 99% confidence levels. In contrast, the IgFLNa10 difference densities fall outside the boundaries of F-actin control reconstructions (Fig. 3c and d).

Despite the relatively low number of filaments in half-data sets of F-actin–IgFLNa10, IgFLNa10 is still readily detected on actin subdomain 1 in reconstructions generated from such divided data (Fig. 2c and d, arrows). In fact, the IgFLNa10 density is a consistent feature of reconstructions of individual filaments of the data set. In addition, a small extra density derived from IgFLNa10 is occasionally detected on subdomains 3 and 4 on the inner border of actin (Fig. 2b and d, open arrows).

Molecular docking of IgFLNa10

Docking atomic models of F-actin[30] into the reconstructions of IgFLNa10-decorated filaments leaves considerable density over the N-terminus of F-actin unoccupied (Fig. 4). The remaining volume can be largely accommodated by the crystal structure of IgFLNa10,[31] which fits snugly into the remaining space (Fig. 4). However, the polarity and sidedness of the Ig structure in the reconstruction are indeterminate, since neither the atomic model of IgFLNa10 nor the EM maps provide sufficient landmarks or asymmetries that can be used to match respective geometrical features with precision. In fact, the extra volume attributable to IgFLNa10 binding is about 30% broader than the

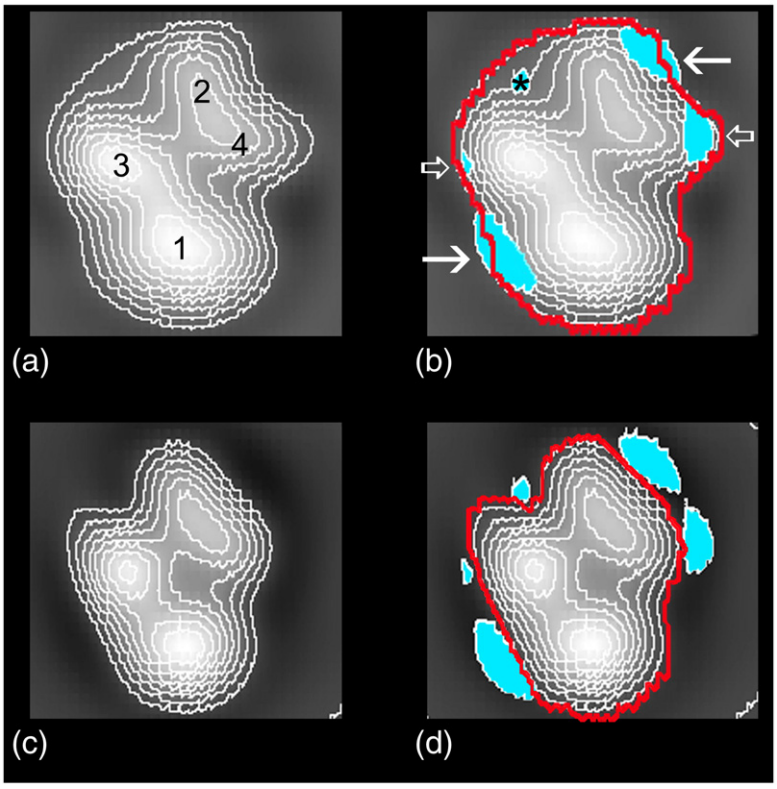

Fig. 3. Statistical significance of IgFLNa10 densities in the F-actin–IgFLNa10 reconstruction. (a) Transverse (z-)section taken through F-actin–IgFLNa10 at the level indicated by the arrows shown in Fig. 2b. Actin subdomain locations in the z-section are marked in (a). (b) z-section in (a) superposed with difference densities representing the contribution of IgFLNa10 (cyan). Difference densities were determined by subtracting densities in the F-actin reconstruction from those in F-actin–IgFLNa10. Densities in the F-actin–IgFLNa10 reconstruction that are significant at greater than the 95% confidence level are encircled by a red tracing and include the difference densities. Large arrows indicate the IgFLNa10 density that caps actin subdomain 1 and projects over subdomain 2. Open arrows indicate small pointed density on subdomains 3 and 4 (noted in Fig. 2). Asterisk indicates difference density likely to be due to staining differences between samples. (c) Transverse section of pure F-actin and (d) F-actin superposed with the above FLNaIg10 difference densities. Those densities that are significant in the F-actin map at greater than the 95% confidence level are encircled by a red tracing. Note that the IgFLNa10 difference densities fall outside of this map. Statistical significance was computed from the variances associated with each contributing point in the reconstructions according to Milligan and Flicker[35] and Trachtenberg and DeRosier.[36]

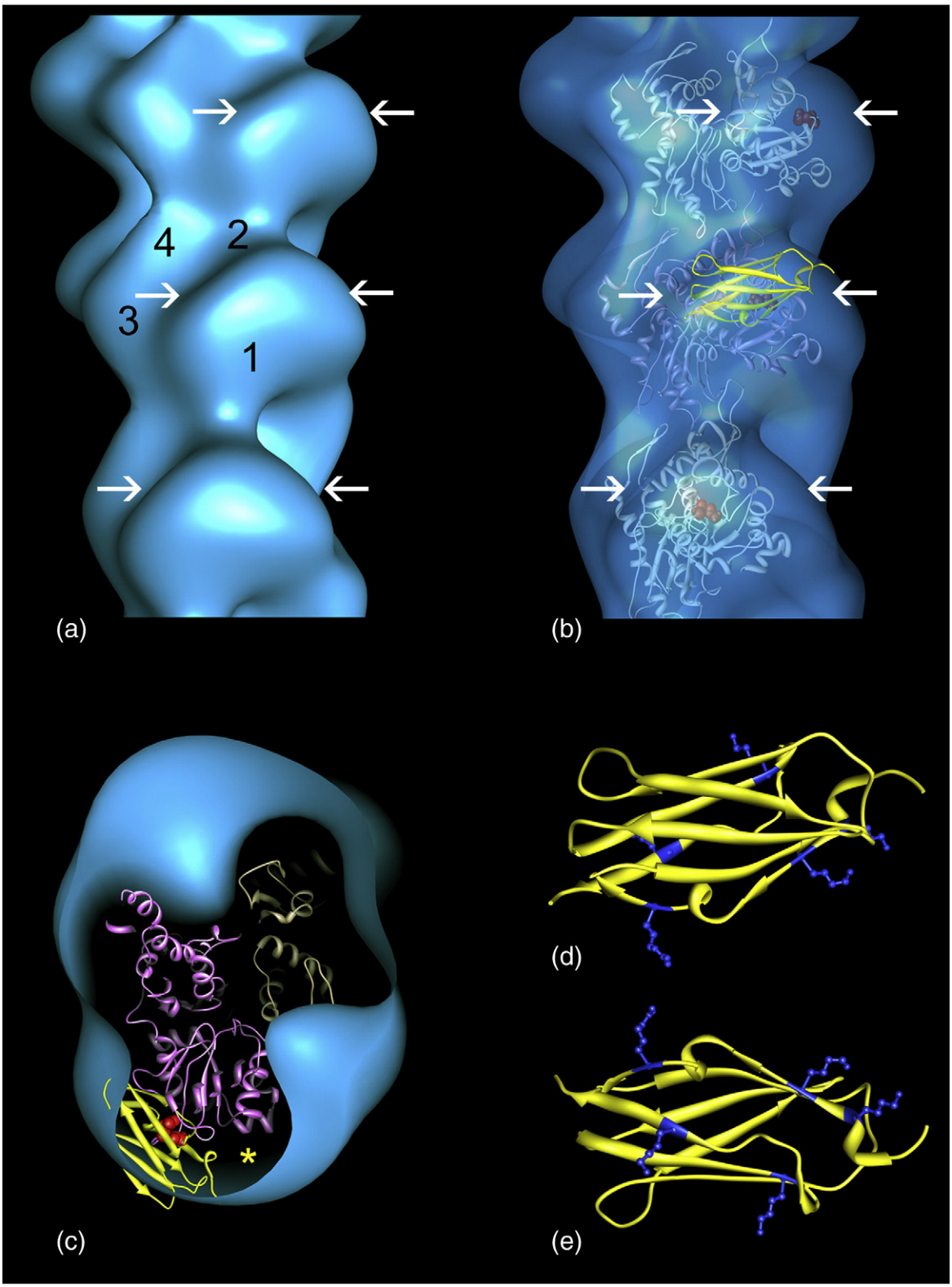

Fig. 4 (*legend on next page*)

dimensions of the crystal structure, suggesting azimuthal variance in the localization of the Ig repeat on the surface of actin (Fig. 4c).

The N-terminus of actin contains a string of negatively charged amino acids. If electrostatic interactions with the actin N-terminus are a driver of IgFLNa10 actin binding, then only one interface of the IgFLNa10 structure contains a suitable binding surface of complementary basic residues and includes Lys1162, Lys1164, Arg1172, Lys1234, and Lys1246 (cf., Protein Data Bank ID 3rgh).[31] Interestingly, these residues outline a groove on IgFLNa10 that may be the target for the actin's acidic residues (Fig. 4). Indeed, the N-terminal residues on actin represent one of the least conserved regions of this otherwise stringently conserved molecule,[37] suggesting that actin isoform and Ig-repeat specificity may account for filamin sorting to one or another cell cytoskeletal domain. However, many of these basic amino acids are themselves conserved in the other Ig repeats including IgFLNa9, IgFLNa17, and IgFLNa16–23, which do not interact with F-actin, suggesting that neighboring residues, in addition to these basic amino acids, play a role in mediating this interaction or in producing a preference for solvent. Higher-resolution structures are necessary to resolve this interface in greater detail. Further studies are also necessary to determine how the disease-causing mutations affect the structure of IgFLNa10 and whether they alter its F-actin interaction.

Conclusions

The studies reported here directly reveal an Ig domain–F-actin interaction structurally for the first time. Despite relatively low sequence similarity, members of the Ig-domain superfamily are structurally related by a common “Ig-fold” consisting of two sheets of antiparallel β-strands that are sandwiched together.[16] Given that Ig domains have varied amino acid sequences, it is not surprising that only certain FLNa Ig modules, in the case of our studies, Ig10FLNa, bind to F-actin with demonstrable affinity. Nevertheless, we cannot exclude the possibility that macromolecular crowding in a cellular environment may increase the effective concentration of other FLNa Ig modules sufficiently to favor actin interactions that went undetected under our conditions *in vitro*.

Based on the current and previous work, we propose a model of FLNa cytoskeletal interaction in which neighboring but weakly interacting CH and Ig domains cooperatively promote FLNa binding to F-actin. This process then repeats itself as FLNa populates F-actin and cross-links adjoining filaments to form a mechanically cohesive network. However, because local FLNa–actin interactions are weak, chemical or mechanical signaling can easily perturb these networks during cytoskeletal remodeling. The general binding strategy discussed here, in which an elongated molecule utilizes multiple well-separated but weakly interacting domains to bind to F-actin, is not limited just to filamin-binding function but may also operate in myosin-binding protein C–thin filament association, where multiple Ig repeats and the M-motif appear to reinforce each other during thin filament binding.[20,21] Similarly, in the case of elongated dystrophin and utrophin, spectrin repeats distal to CH domains may enhance actin binding.[27,38–40] In fact, the well-established formula for tropomyosin binding to thin filaments involves multiple weakly interacting pseudo-repeats linked to successive actin subunits along filaments.[28,41] Thus, actin network patterning based on tandem weakly interacting protein domains may be a commonly used strategy to style the fabric of the actin cytoskeleton.

Acknowledgements

This work was supported by National Institutes of Health Program Project Grants P01 HL86655 to Kathleen G. Morgan (W.L., principal investigator), R01 HL036153 to W.L., and R01 HL089224 to J.H.H., and the Harvard University Science and Engineering Committee Seed Fund for Interdisciplinary Science to F.N.

Fig. 4. Fitting the crystal structure model of IgFLNa10 into the IgFLNa10–F-actin reconstruction. (a) F-actin–IgFLNa10 reconstruction and (b) reconstruction made translucent and fitted with the Oda/Maeda atomic model of F-actin[30] (in ribbon format) and then with the crystal structure of IgFLNa10 (yellow, Protein Data Bank ID 3rgh)[31] into the remaining volume of one actin subunit. The IgFLNa10 structure was centered over the N-terminus of F-actin (noted by red aspartate residue). (c) Cross-section of the fitted reconstruction viewed from the barbed end of the filament, showing the volume occupied by actin (magenta and olive drab) and IgFLNa10 (yellow); adjacent unoccupied volume is indicated by an asterisk. In (b) and (c), basic amino acids on IgFLNa10 were oriented facing toward actin. (d) An enlargement of IgFLNa10 as it was oriented in (b) highlighting the basic amino acids of IgFLNa10 (light blue). (e) One hundred eighty-degree rotation of IgFLNa10 in (d) showing the basic amino acids en face. These residues outline a groove that might be a target for the N-terminal acidic amino acids of F-actin. The docking of atomic models into the reconstruction volume was performed with Chimera fitting tools.[32]

Received 14 August 2012;
Received in revised form 24 September 2012;
Accepted 28 September 2012
Available online 4 October 2012

Keywords:
actin;
filamin;
cytoskeleton;
electron microscopy;
3D reconstruction

Abbreviations used:
ABD, actin-binding domain; CH, calponin homology; EM, electron microscopy; FLNa, filamin A; IgFLNa, immunoglobulin-like filamin A repeat; 3D, three-dimensional.

References

1. Stossel, T. P., Fenteany, G. & Hartwig, J. H. (2006). Cell surface actin remodeling. *J. Cell Sci.* **119**, 3261–3264.
2. Pollard, T. D. & Cooper, J. A. (2009). Actin, a central player in cell shape and movement. *Science*, **326**, 1208–1212.
3. Ridley, A. J. (2011). Life at the leading edge. *Cell*, **145**, 1012–1022.
4. dos Remedios, C. G., Chhabra, D., Kekic, M., Dedova, I. V., Tsubakihara, M., Berry, D. A. & Nosworthy, N. J. (2003). Actin binding proteins: regulation of cytoskeletal microfilaments. *Physiol. Rev.* **83**, 433–473.
5. Hartwig, J. H. & Stossel, T. P. (1975). Isolation and properties of actin, myosin, and a new actin binding protein in rabbit alveolar macrophages. *J. Biol. Chem.* **250**, 5696–5705.
6. Hartwig, J. H. & Stossel, T. P. (1981). Structure of macrophage actin-binding protein molecules in solution and interacting with actin filaments. *J. Mol. Biol.* **145**, 563–581.
7. Gardel, M. L., Nakamura, F., Hartwig, J. H., Crocker, J. C., Stossel, T. P. & Weitz, D. A. (2006). Prestressed F-actin networks cross-linked by hinged filamins replicate mechanical properties of cells. *Proc. Natl Acad. Sci. USA*, **103**, 1762–1767.
8. Nakamura, F., Osborn, T. M., Hartemink, C. A., Hartwig, J. H. & Stossel, T. P. (2007). Structural basis of filamin A functions. *J. Cell Biol.* **179**, 1011–1025.
9. Gardel, M. L., Kasza, K. E., Brangwynne, C. P., Liu, J. & Weitz, D. A. (2008). Mechanical response of cytoskeletal networks. *Methods Cell Biol.* **89**, 487–519.
10. Nakamura, F., Stossel, T. P. & Hartwig, J. H. (2011). The filamins: organizers of cell structure and function. *Cell Adh. Migr.* **5**, 160–169.
11. Ehrlicher, A. J., Nakamura, F., Hartwig, J. H., Weitz, D. A. & Stossel, T. P. (2011). Mechanical strain in actin networks regulates FilGAP and integrin binding to filamin A. *Nature*, **478**, 260–263.
12. Stradal, T., Kranewitter, W., Winder, S. J. & Gimona, M. (1998). CH domains revisited. *FEBS Lett.* **431**, 134–137.
13. Gorlin, J. B., Yamin, R., Egan, S., Stewart, M., Stossel, T. P., Kwiatkowski, D. J. & Hartwig, J. H. (1990). Human endothelial actin-binding protein (ABP-280, nonmuscle filamin): a molecular leaf spring. *J. Cell Biol.* **111**, 1089–1105.
14. Ruskamo, S., Gilbert, R., Hofmann, G., Jiang, P., Campbell, I. D., Ylänne, J. & Pentikainen, U. M. (2012). The C-terminal rod 2 fragment of filamin A forms a compact structure that can be extended. *Biochem. J.* **446**, 261–269.
15. Tossavainen, H., Koskela, O., Jiang, P., Ylänne, J., Campbell, I. D., Kilpeläinen, I. & Permi, P. (2012). *J. Am. Chem. Soc.* **134**, 6660–6672.
16. Otey, C. A., Dixon, R., Stack, C. & Goicoechea, S. M. (2009). Cytoplasmic Ig-domain proteins: cytoskeletal regulators with a role in human disease. *Cell Motil. Cytoskeleton*, **66**, 618–634.
17. Dixon, R. D. S., Arneman, D. K., Rachlin, A. S., Sundaresan, N., Costello, J. M., Campbell, S. L. & Otey, C. A. (2008). Palladin is an actin crosslinking protein that uses immunoglobulin-like domains to bind filamentous actin. *J. Biol. Chem.* **283**, 6222–6231.
18. Bullard, B., Garcia, T., Benes, V., Leake, M. C., Linke, W. A. & Oberhauser, A. F. (2006). The molecular elasticity of the insect flight muscle proteins projectin and kettin. *Proc. Natl Acad. Sci. USA*, **103**, 4451–4456.
19. Ono, K., Yu, R., Mohri, K. & Ono, S. (2006). *Caenorhabditis elegans* kettin, a large immunoglobulin-like repeat protein, binds to filamentous actin and provides mechanical stability to the contractile apparatuses in body wall muscle. *Mol. Biol. Cell*, **17**, 2722–2734.
20. Shaffer, J. F., Kensler, R. W. & Harris, S. P. (2009). The myosin-binding protein C motif binds to F-actin in a phosphorylation-sensitive manner. *J. Biol. Chem.* **284**, 12318–12327.
21. Mun, J. Y., Gulick, J., Robbins, J., Woodhead, J., Lehman, W. & Craig, R. (2011). Electron microscopy and 3D reconstruction of F-actin decorated with cardiac myosin-binding protein C (cMyBP-C). *J. Mol. Biol.* **410**, 214–225.
22. Oakley, C. E., Chamoun, J., Brown, L. J. & Hambly, B. D. (2007). Myosin binding protein-C: enigmatic regulator of cardiac contraction. *Int. J. Biochem. Cell Biol.* **39**, 2161–2166.
23. Tskhovrebova, L. & Trinick, J. (2004). Properties of titin immunoglobulin and fibronectin-3 domains. *J. Biol. Chem.* **279**, 46351–46354.
24. Robertson, S. P., Jenkins, Z. A., Morgan, T., Adès, L., Aftimos, S., Boute, O. *et al.* (2006). Frontometaphyseal dysplasia: mutations in FLNA and phenotypic diversity. *Am. J. Med. Genet. A*, **140**, 1726–1736.
25. Spudich, J. A. & Watt, S. (1971). The regulation of rabbit skeletal muscle contraction. I. Biochemical studies of the interaction of the tropomyosin-troponin complex with actin and the proteolytic fragments of myosin. *J. Biol. Chem.* **246**, 4866–4871.
26. Moody, C., Lehman, W. & Craig, R. (1990). Caldesmon and the structure of smooth muscle thin filaments: electron microscopy of isolated thin filaments. *J. Muscle Res. Cell Motil.* **11**, 176–185.
27. Sutherland-Smith, A. J., Moores, C. A., Norwood, F. L., Hatch, V., Craig, R., Kendrick-Jones, J. & Lehman, W. (2003). An atomic model for actin binding by the CH domains and spectrin-repeat modules of utrophin and dystrophin. *J. Mol. Biol.* **329**, 15–33.

28. Li, X. E., Tobacman, L. S., Mun, J. Y., Craig, R., Fischer, S. & Lehman, W. (2011). Tropomyosin position on F-actin revealed by EM reconstruction and computational chemistry. *Biophys. J.* **100**, 1005–1013.
29. Owen, C., Morgan, D. G. & DeRosier, D. J. (1996). Image analysis of helical objects: the Brandeis Helical Package. *J. Struct. Biol.* **116**, 167–175.
30. Oda, T., Iwasa, M., Aihara, T., Maéda, Y. & Narita, A. (2009). The nature of the globular- to fibrous-actin transition. *Nature*, **457**, 441–445.
31. Page, R. C., Clark, J. G. & Misra, S. (2011). Structure of filamin A immunoglobulin-like repeat 10 from *Homo sapiens*. *Acta Crystallogr., Sect. F*, **67**, 871–876.
32. Pettersen, E. F., Goddard, T. D., Huang, C. C., Couch, G. S., Greenblatt, D. M., Meng, E. C. & Ferrin, T. E. (2004). UCSF Chimera—a visualization system for exploratory research and analysis. *J. Comput. Chem.* **25**, 1605–1612.
33. Orlova, A. A., Galkin, V. E., Nakamura, F. & Egelman, E. H. (2011). Filamin CH domains bind to F-actin in an open conformation. *Mol. Biol. Cell*, **22**, 794a.
34. Nakamura, F., Osborn, E., Janmey, P. A. & Stossel, T. P. (2002). Comparison of filamin A-induced cross-linking and Arp2/3 complex-mediated branching on the mechanics of actin filaments. *J. Biol. Chem.* **277**, 9148–9154.
35. Milligan, R. A. & Flicker, P. F. (1987). Structural relationships of actin, myosin, and tropomyosin revealed by cryo-electron microscopy. *J. Cell Biol.* **105**, 29–39.
36. Trachtenberg, S. & DeRosier, D. J. (1987). Three-dimensional structure of frozen hydrated flagellar filament of *Salmonella typhimurium*. *J. Mol. Biol.* **195**, 581–601.
37. Lehman, W., Craig, R. & Barany, M. (1996). Actin and the structure of smooth muscle thin filaments. In *Biochemistry of Smooth Muscle Contraction* (Barany, M., ed.), pp. 47–60, Academic Press, San Diego: Inc.
38. Amann, K. J., Renley, B. A. & Ervasti, J. M. (1998). A cluster of basic repeats in the dystrophin rod domain binds F-actin through an electrostatic interaction. *J. Biol. Chem.* **273**, 28419–28423.
39. Rybakova, I. N., Humston, J. L., Sonnemann, K. J. & Ervasti, J. M. (2006). Dystrophin and utrophin bind actin through distinct modes of contact. *J. Biol. Chem.* **281**, 9996–10001.
40. Henderson, D. M., Lin, A. Y., Thomas, D. D. & Ervasti, J. M. (2012). The carboxy-terminal third of dystrophin enhances actin binding activity. *J. Mol. Biol.* **416**, 414–424.
41. Holmes, K. C. & Lehman, W. (2008). Gestalt-binding of tropomyosin to actin filaments. *J. Muscle Res. Cell Motil.* **29**, 213–219.